

Surface Tension Measurements of Liquid Metals Using Levitation, Microgravity, and Image Processing¹

I. Egry,² G. Lohöfer,² P. Neuhaus,² and S. Sauerland²

An improved method for measuring the surface tension of liquid metals is proposed. It makes use of the electromagnetic levitation technique for levitating a liquid metal droplet and of digital image processing to evaluate the surface oscillations of the droplet. The oscillation frequencies determine the surface tension. This paper contains a discussion of the theoretical background and a description of the experimental setup. In addition, preliminary results on FeNi samples in 1g and microgravity are presented.

KEY WORDS: image processing; levitation; microgravity; metals; surface tension.

1. INTRODUCTION

The measurement of thermophysical properties is a continuous activity of many research groups. Data on thermophysical properties are needed not only to plan, conduct, and control many technological processes but also to provide a firm ground for our understanding of the basic physics.

Among these, the surface tension of liquid metals is a particularly interesting quantity. At a liquid-vapor interface, the density changes drastically from a high value in the liquid state to a very low value in the gas phase. Consequently, surface atoms experience a net attraction toward the liquid, which is the origin of the surface tension. Obviously, the density is the key parameter in determining the surface tension. The appropriate theoretical framework is the density functional theory [1, 2], which has made considerable progress in recent years, yielding realistic values for the

¹ Paper presented at the Second Workshop on Subsecond Thermophysics, September 20–21, 1990, Torino, Italy.

² Institute for Space Simulation, German Aerospace Research Establishment, DLR, 5000 Köln-90, Germany.

simple alkali metals. For finite temperatures, entropic contributions to the surface tension [3] must also be taken into account.

Liquid metals are difficult to handle due to the high temperatures involved and their high reactivity. In particular, they tend to oxidize which dramatically changes optical, thermal and mechanical properties of the surface. A convenient way for measuring the surface tension of liquid metals is the use of electromagnetic levitation. This method avoids any contact with a crucible and reduces systematic errors due to surface contamination inherent in alternative techniques, such as the sessile-drop technique [4]. Furthermore, it allows deep undercooling of the liquid metal [5]. In addition, electromagnetic levitation can be used to measure the density of liquid metals, the earliest example being nickel [6]. Measurements of the surface tension using this techniques have been first carried out by Fraser et al. [7] and, more recently, by Schade et al. [8], Keene et al. [9] and Nogi et al. [10]. The surface tension is measured by exciting shape oscillations of the liquid sample and determining their frequencies. Fraser et al. [7] used high-speed cinematography for recording the surface oscillations, while the latter groups employed a photodiode to record the incoming light intensity. However, the photodiode yields only the intensity, which is an integrated signal and contains no information about the actual type of oscillation. This is a serious problem in terrestrial measurements. Due to the action of gravity, levitated samples become aspherical upon melting. As is well known [11], aspherical drops have a complicated frequency spectrum manifested by three or more peaks. In order to attribute peaks in the frequency spectrum to the corresponding normal modes, the actual type of the oscillation must be known. This complication does not arise in microgravity where the liquid sample remains spherical. We have therefore proposed a microgravity experiment for measuring surface tension and viscosity of undercooled metallic melts [12].

In this paper, we present preliminary results on a comparison between a spectrum taken in microgravity and a spectrum taken on earth. As expected, the ground-based spectrum shows three peaks, whereas the microgravity spectrum shows one peak only. We have analyzed experiments which were performed during parabolic flights of a KC-135 aircraft providing about 10 s of microgravity. These flights were intended primarily to test TEMPUS, an electromagnetic levitation facility designed to operate in microgravity. Accordingly, the experimental conditions were far from optimal, but we were able to melt an FeNi sample and to excite and observe oscillations. For comparison, we have repeated the measurements using a ground-based levitation facility [13].

In contrast to the previously mentioned groups, we record the oscillations by a video camera and use subsequent digital image processing. This

has the advantage that the images contain the full (two-dimensional) information and can be analyzed for shape and frequency. Liggieri and Passerone [14] have also applied image processing routines for measuring the surface tension of liquid metals via the sessile drop technique. They analyze static images and it is the spatial resolution of the video camera which is the limiting factor. On the other hand, the oscillating drop technique is a dynamical one, and therefore, the temporal resolution is a problem. Conventional video cameras use two interlaced half-frames at 50 Hz. Depending on the mass of the sample, the oscillation frequencies lie in the range between 10 and 100 Hz. It is therefore essential to increase the sampling rate of the video camera. An increase by a factor n can be achieved if one reads only a fraction $1/n$ ($n = 2, \dots, 10$) of the frame. We have used $n = 1$ (50 Hz) in the microgravity experiment and $n = 3$ (150 Hz) on the ground. In comparison with the sampling rate of a photodiode system, which, including A/D-conversion, can be in the megahertz range [15], the low sampling rate is the major drawback of the video system.

2. DROP OSCILLATIONS

Surface tension and viscosity can be measured by detecting surface oscillations of a levitated drop. The frequency ν of the oscillations is related to the surface tension σ , while the damping γ yields the viscosity η . The theory of oscillations of a liquid drop is a classical problem in hydrodynamics [16] and has been treated to several degrees of sophistication. In its simplest version, the theory deals with free linear oscillations of inviscid, nongravitating spherical drops. It has also been treated as an initial-value problem [17] and as forced oscillation [18]. Subsequently, the influence of viscosity [19], self-gravity [20], nonlinearity [21], and asphericity [11] has been taken into account. For our purposes, it is sufficient to consider the linear oscillations of an inviscid, aspherical drop. The measurement of viscosity by the same method has been discussed elsewhere [12].

The radius of a spherical droplet undergoes oscillations of the form

$$R_l \sim \cos(2\pi\nu_l t) P_l(\cos \vartheta) \quad (1)$$

where ϑ is the angle with respect to the symmetry axis, l is an integer labeling the normal modes, and P_l is a Legendre polynomial. In the linearized theory [16], the frequencies ν_l are given by

$$\nu_l^2 = \frac{1}{3\pi} l(l-1)(l+2) \frac{\sigma}{M} \quad (2)$$

where M is the mass of the sphere. The fundamental mode is $l = 2$.

For this mode, Cummings and Blackburn [11] have calculated the effect of asphericity and sample rotation. The main result of their calculation is that the frequency of the fundamental $l=2$ -mode is shifted and split into as many as five sidebands. This is due to the fact that Eq. (1) is not the most general solution for aspherical drops. Allowing for azimuthal dependence, it is given by

$$R_{l,m} \sim \cos(2\pi\nu_{l,m}t) P_l^m(\cos \vartheta) \cos[m(\varphi - \varphi_0)] \quad (3)$$

where φ_0 is a constant, $|m| \leq l$, and P_l^m is an associated Legendre function.

For a nonrotating axisymmetric droplet, the frequencies depend on $|m|$ only, and one expects three peaks of the $l=2$ -mode. These are given in Ref. 11 by

$$\nu_{2,0} = \nu_2(1 - 0.6758 \alpha - 2.176 \beta) \quad (4)$$

$$\nu_{2,1} = \nu_2(1 - 0.3379 \alpha + 1.451 \beta) \quad (5)$$

$$\nu_{2,2} = \nu_2(1 + 0.6758 \alpha - 0.363 \beta) \quad (6)$$

where α and β are two parameters describing the asphericity of the sample's equilibrium shape. They depend on the gravity and surface tension of the sample and are essentially unknown. If the correct assignment of the frequency peaks is not possible, Eqs. (4), (5), and (6) do not allow the determination of ν_2 and hence the surface tension σ . However, Cummings and Blackburn [11] have derived a sum rule which can be used to estimate ν_2 from a triply split spectrum. They also included the effect of translational oscillations of the sample as a whole. Their result is

$$\nu_2^2 = \frac{1}{10} (3\nu_{\max}^2 + 3\nu_{\min}^2 + 4\nu_{\text{middle}}^2) - 2\nu_t^2 \pm \frac{1}{10} (\nu_{\max}^2 - \nu_{\min}^2) \quad (7)$$

where ν_t is the translational frequency. Comparing Eq. (7) with Eq. (2) it is evident that oscillations of spherical drops are much easier to evaluate. This possibility is offered by the microgravity environment.

3. IMAGE PROCESSING

A video camera produces two-dimensional images which are projections of the sample onto a plane normal to the viewing direction. Sample oscillations are detected as variations in the shape of these images. It is convenient to binarize the images choosing a suitable threshold such that the sample will be displayed white, whereas the remainder of the picture will be black. This step eliminates the effect of temperature on the signal

and suppresses any unwanted reflections. A number of methods can be applied to relate the binary images to the sample oscillations. One way is to determine directly the radius at a fixed angle ϑ_0 for each frame. According to Eq. (3), the temporal change of this quantity yields directly frequency and damping. If the sample undergoes translational oscillations, i.e., the position R_{CM} of the center of mass varies in a laboratory frame of reference according to

$$R_{CM} \sim \cos(2\pi\nu_t t) \quad (8)$$

the apparent change in radius is the sum of translational and vibrational motion. By compensating for the translation and by choosing the appropriate angle, one can suppress signals from certain modes. For example,

$$P_2^0[\cos(54.7^\circ)] = 0 \quad (9)$$

while $P_2^m \neq 0$ for $m = 1, 2$.

Another possibility is to use the area of the cross section Q as the signal. For a side view (perpendicular to the symmetry axis), one obtains [22] in first order,

$$Q_{l,m}^{\text{side}}(t) = \pi R_0^2 \left\{ 1 + \varepsilon \cos(2\pi\nu_{l,m} t) \frac{2}{\pi} \int_0^\pi d\vartheta P_l^m(\cos \vartheta) \right\} \quad (10)$$

where ε is the amplitude of the oscillation. For $(l-m)$ odd, the integral vanishes yielding a selection rule.

When viewing from the top (along the symmetry axis), the corresponding result is [22]

$$Q_{l,m}^{\text{top}}(t) = \pi R_0^2 \{ 1 + 2\varepsilon \cos(2\pi\nu_{l,m} t) P_l^m(0) \delta_{m,0} \} \quad (11)$$

which implies that only the $m=0$ -mode causes a variation in the equatorial cross section and hence a detectable signal. It must be noted, however, that these selection rules are valid only as long as the total cross section remains visible, which in practice is not the case. Under the same assumption, this analysis is insensitive to translational oscillations of the sample. The frequencies $\nu_{l,m}$ are obtained by Fourier transforming the signal.

In order to derive surface tension values from measured frequency spectra, one must assign the correct labels (l, m) to each peak in the spectrum. Presently, this is done by visual inspection of the images frame by frame and choosing only those parts of the sequence for frequency analysis where the sample oscillates in only one unambiguously identified mode. For the future, more sophisticated methods are in preparation.

4. EXPERIMENT

4.1. Levitation Under 1g

The terrestrial measurements have been performed in a conventional levitation facility, as described in Ref. 13. A generator operating at 330 kHz is connected to a conical coil which provides levitation and heating. Temperature is measured by a two-color ratio pyrometer. In contrast to microgravity levitation, only relatively small samples ($M \approx 1g$) can be processed. This leads to oscillation frequencies in the 40-Hz range [see Eq. (2)]. According to the Nyquist theorem [23], a sampling frequency of at least 80 Hz is therefore necessary. As mentioned in Section 1, standard video cameras have a 50-Hz sampling rate. We have therefore used a modified video camera which increases sampling rates by a factor n by reading only $1/n$ lines of each frame. We have taken $n=3$, equivalent to 150 Hz, which is a reasonable compromise between spatial and temporal resolution.

The images were recorded on a S-VHS video recorder and analyzed off-line. For frequency analysis, we evaluated the lateral cross-sectional area $Q(t)$ [Eq. (10)] for 256 images. The resulting signal, $Q(t)$, is then Fourier transformed to obtain the linear frequency spectrum. The frequency spectrum for an $Fe_{90}Ni_{10}$ sample at $T \approx 1520^\circ C$ is shown in Fig. 1. Two low-lying peaks due to translational motion of the sample and the triply

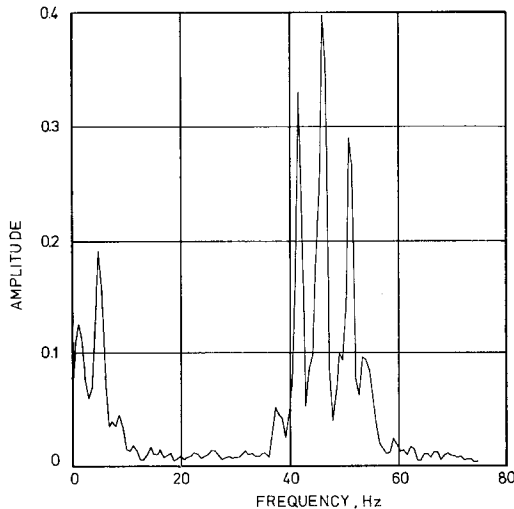


Fig. 1. Fourier spectrum for an oscillating sphere of $Fe_{90}Ni_{10}$ in 1g.

split $l=2$ -mode can be seen. It was not possible to identify the individual m -labels, and therefore Eq. (7) was used to estimate the surface tension. Rewriting Eq. (2) for $l=2$ we obtain

$$\sigma = \frac{3}{8}\pi Mv_2^2 \quad (12)$$

where M is the mass of the sample. Inserting $M=0.71\text{g}$, we find for the surface tension $\sigma = 1.76 \pm 0.06 \text{ N}\cdot\text{m}^{-1}$, in fair agreement with values reported in the literature [24]; these are in the range between 1.7 and $1.8 \text{ N}\cdot\text{m}^{-1}$.

4.2. Microgravity Levitation

These experiments were carried out in the development model of the TEMPUS facility, shown schematically in Fig. 2. TEMPUS uses a two-coil, two-frequency concept which allows the heating (dipole) field and the positioning (quadrupole) field to be varied independently. A short voltage pulse through the heating coil can be used to excite the surface oscillations.

TEMPUS is equipped with a two-color pyrometer with a measuring range of $300\text{--}2400^\circ\text{C}$ and a sampling rate of 1 MHz. Two video cameras

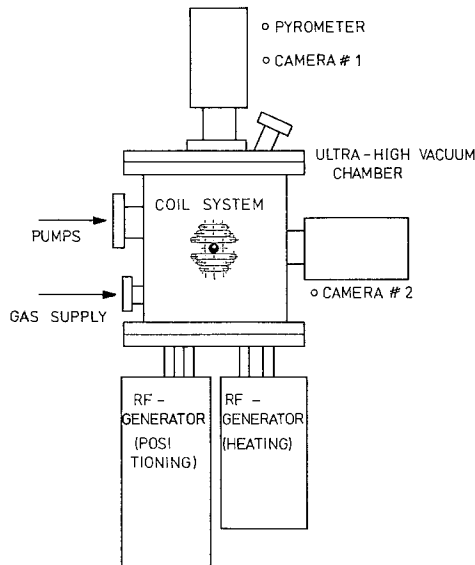


Fig. 2. Schematic view of TEMPUS, showing the camera positions.

(50 Hz monochrome) offer top and side view. The facility can operate under an inert purified gas atmosphere (Ar, He) or ultrahigh vacuum (10^{-9} mbar). Spherical samples with radius $R_0 = 5$ mm can be processed.

TEMPUS cannot levitate against $1g$. Therefore, it had to be tested during parabolic flights on a KC-135 airplane. Each parabola provides about 10 s of $10^{-2}g$. The original intention was to test the positioning capabilities of TEMPUS only. It turned out, however, that the time was sufficient to position and melt the sample and to excite surface oscillations. An $\text{Fe}_{75}\text{Ni}_{25}$ sample with a mass of 4.2 g was used and processed in a helium atmosphere.

We used Eq. (10) to obtain the signal $Q(t)$. The variation of $Q(t)$ during the first 4 s is shown in Fig. 3. In the first 2 s of the experiment, the sample is solid and shows no oscillation. It is then heated above its melting point up to $T \approx 1580^\circ\text{C}$ and oscillations are excited at about $t = 3$ s. The oscillations stop at about $t = 6$ s when gravity sets in again and the sample hits the sample holder.

For the frequency analysis, only that part of the signal free from transient disturbances was used. The Fourier transform of 128 images is shown in Fig. 4. In addition to some low-frequency peaks, which can be attributed to translational motion of the sample, it has one sharp peak at $\nu = 17.8$ Hz. We identified this peak as the $(l=2, m=0)$ -mode by visual inspection of the video recordings. The appearance of only one peak is due to the fact that the sample remains essentially spherical in microgravity.

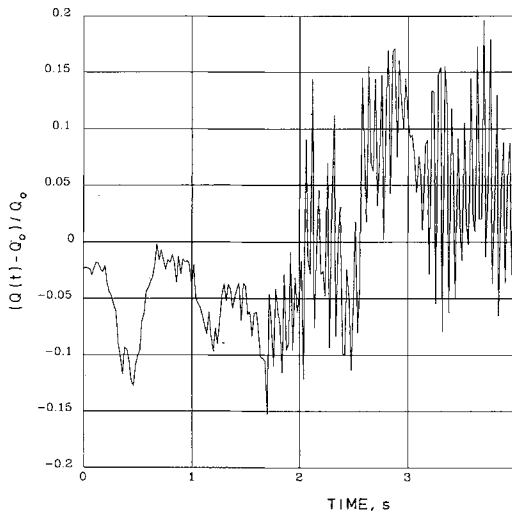


Fig. 3. Signal $Q(t)$ versus time for an oscillating sphere of $\text{Fe}_{90}\text{Ni}_{10}$ in micrograms. Q_0 is the mean value of $Q(t)$.

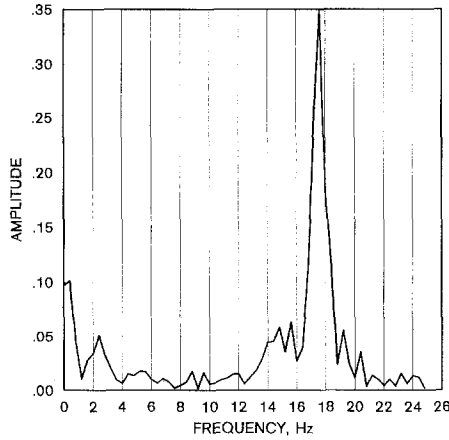


Fig. 4. Fourier spectrum for an oscillating sphere of $\text{Fe}_{75}\text{Ni}_{25}$ in micrograms.

It should also be mentioned that the peak at 17.8 Hz does not appear in the oscillation spectrum of the solid sample, indicating that it is not an artifact of the analysis, but a genuine property of the surface oscillations of the liquid sample. Inserting $M = 4.2g$ into Eq. (12), we obtain $\sigma = 1.6 \text{ N} \cdot \text{m}^{-1}$. For $\text{Fe}_{76}\text{Ni}_{24}$, a composition very similar to that of our sample, a surface tension value of $\sigma = 1.68 \text{ N} \cdot \text{m}^{-1}$, essentially independent of temperature, is listed in Ref. 24. The agreement is satisfactory, taking the restricted experimental conditions into account. For example, the purity of the sample, the experiment duration, the resolution of the video system, and finally, the temperature measurement were not of the standard which we are used to in our laboratory. We want to stress, however, that the major achievement of our result is not its numerical value, but the fact that we obtained essentially a single peaked spectrum, which eliminates systematic errors due to incorrect or uncertain peak assignment. A high-precision measurement of σ in microgravity is the subject of our experiment proposal for the Spacelab mission IML-2 [12].

5. CONCLUSIONS

Electromagnetic levitation is a very powerful tool to measure thermophysical properties of liquid metals such as surface tension and viscosity. Presently, the precision of this method when used on the ground is limited by the fact that an unambiguous mode assignment is not possible for multiply peaked spectra. Carrying out the experiments under

microgravity conditions yields spherical samples, and hence, no frequency splitting occurs. In addition, shape analysis via image processing allows an assignment of peaks even in more complicated spectra.

ACKNOWLEDGMENTS

Thanks are due to J. Piller and R. Knauf from Dornier GmbH, who participated in the experiment on the KC-135 flight. We also thank D. Cummings, who made the work on aspherical drops available to us prior to publication.

REFERENCES

1. N. D. Lang, in *Solid State Phys.* **28**:225 (1973).
2. D. Stroud and M. J. Grimson, *J. Non Crystal. Solids* **68**:231 (1984).
3. F. Spaepen and R. B. Meyer, *Scripta Metallurg.* **10**:257 (1976).
4. R. Sangiorgi, G. Caracciolo, and A. Passerone, *J. Mater. Sci.* **17**:2895 (1982).
5. R. Willnecker, D. M. Herlach, and B. Feuerbacher, *Appl. Phys. Lett.* **49**:1339 (1986).
6. S. Y. Shiraishi and R. G. Ward, *Can. Metallurg. Q.* **3**:117 (1964).
7. M. E. Fraser, W.-K. Lu, A. E. Hamielec, and R. Murarka, *Metallurg. Trans.* **2**:817 (1971).
8. J. Schade, A. McLean, and W. A. Miller, *Undercooled Alloy Phases*, Proceedings 115th Annual Meeting of TMS-AIME, E. W. Collins and C. C. Koch, eds. (1986), p. 233.
9. B. J. Keene, K. C. Mills, A. Kasama, A. McLean, and W. A. Miller, *Metallurg. Trans.* **17B**:159 (1986).
10. K. Nogi, K. Ogino, A. McLean, and W. A. Miller, *Metallurg. Trans.* **17B**:163 (1986).
11. D. L. Cummings and D. A. Blackburn, *J. Fluid Mech.* **224**:395 (1991).
12. I. Egry, B. Feuerbacher, G. Lohöfer, and P. Neuhaus, *ESA SP-295*:257 (1990).
13. D. M. Herlach, R. Willnecker, and F. Gillessen, *ESA SP-222*:399 (1984).
14. L. Liggieri and A. Passerone, *High Temp. Technol.* **7**:82 (1989).
15. E. Schleip, R. Willnecker, D. M. Herlach, and G. P. Görler, *Mater. Sci. Eng.* **98**:39 (1988).
16. H. Lamb, *Hydrodynamics* (Dover, New York, 1945), Chap. IX, Sect. 275.
17. A. Prosperetti, *J. Fluid Mech.* **100**:333 (1980).
18. P. L. Marston, *J. Acoust. Soc. Am.* **67**:15 (1980).
19. W. H. Reid, *Q. Appl. Math.* **18**:86 (1960).
20. A. D. Myshkis, V. G. Babski, N. D. Kopachevskii, L. A. Slobozhanin, and A. D. Tyuptsov, *Low-Gravity Fluid Mechanics* (Springer, Berlin, 1987), p. 398.
21. R. Natarajan and R. A. Brown, *Phys. Fluids* **29**:2788 (1986).
22. I. Egry, *J. Mater. Sci.* **26**:2997 (1991).
23. A. V. Oppenheim and R. W. Schaffer, *Digital Signal Processing* (Prentice-Hall, Englewood Cliffs, NJ, 1975), p. 26.
24. B. J. Keene, *Int. Mater. Rev.* **1**:1 (1988).